

COLLISIONAL RELAXATION OF COLLECTIVE MOTION IN A FINITE FERMI LIQUID

V.M.Kolomietz¹⁾, S.V.Lukyanov¹⁾, V.A.Plujko¹⁾ and S.Shlomo²⁾

¹⁾*Institute for Nuclear Research, Prosp. Nauki 47, 252028 Kiev, Ukraine*

²⁾*Cyclotron Institute, Texas A&M University, College Station, Texas 77843*

Abstract

Finite size effects in the equilibrium phase space density distribution function are taken into account for calculations of the relaxation of collective motion in finite nuclei. Memory effects in the collision integral and the diffusivity and the quantum oscillations of the equilibrium distribution function in momentum space are considered. It is shown that a smooth diffuse (Fermi-type) equilibrium distribution function leads to a spurious contribution to the relaxation time. The residual quantum oscillations of the equilibrium distribution function eliminates the spurious contribution. It ensures the disappearance of the gain and loss terms in the collision integral in the ground state of the system and strongly reduces the internal collisional width of the isoscalar giant quadrupole resonances.

PACS number(s): 21.60.Ev, 24.30.Cz

Typeset using REVTeX

I. INTRODUCTION

The relaxation of nuclear collective motion toward thermal equilibrium have been described in great detail within the framework of the kinetic theory, taking into account the collision integral [1–9]. In this theory, the damping of the collective motion appears due to the interparticle collisions on the dynamically deformed Fermi surface. It has already been shown by Landau [10,11] that both temperature and memory effects are extremely important for successful applications of kinetic theory to the relaxation processes in a Fermi system. However, only very little attention has been paid to the study of the peculiarities of the collision integral in a finite Fermi system caused by particle reflections on the boundary.

In kinetic theory, the collision integral depends crucially on the phase-space distribution function $f(\vec{r}, \vec{p})$. The main aim of this paper is to apply the quantum Wigner phase-space distribution function, also known as the Wigner transform [12], to the evaluation of the collision integral in a finite Fermi system. The Wigner distribution function (WDF) is defined as the Fourier transform of the one-body density matrix over the relative coordinates. It possesses several nice properties [13,14] which justify its interpretation as the quantum mechanical analog of the classical phase-space distribution function. The WDF is useful in providing a reformulation of quantum mechanics in terms of classical concepts [15,16] and a good starting point for semiclassical approximations [17].

Traditionally, the equilibrium phase space density distribution function $f_{eq}(\vec{r}, \vec{p})$ in the collision integral is replaced by the one, $f_{eq,TF}(\vec{r}, \vec{p})$, taken in Thomas-Fermi approximation

$$f_{eq,TF}(\vec{r}, \vec{p}) = \theta(\lambda - E(\vec{r}, \vec{p})), \quad (1)$$

where $\theta(x)$ is the step function and $E(\vec{r}, \vec{p})$ is the classical single-particle energy. This is reasonable for an infinite Fermi system. In the case of a finite Fermi system, the quantum distribution function $f_{eq}(\vec{r}, \vec{p})$ fluctuates strongly and contains the diffusivity of the Fermi surface even at zero temperature [18–23]. Both these features are due to particle reflections on potential walls.

The diffusivity of the Fermi surface in momentum space increases in the vicinity of the nuclear surface [22] and thus enhances the effective particle scattering there because of the decrease of the Pauli blocking effect. It can be shown [9] that the use of a simple Fermi distribution function

$$f_{eq,F}(\vec{r}, \vec{p}) = \left(1 + \exp \left[\frac{E(\vec{r}, \vec{p}) - \lambda}{a(r)} \right] \right)^{-1}, \quad (2)$$

with r -dependent diffusivity parameter $a(r)$, instead of the θ -function of Eq. (1), for the equilibrium distribution function $f_{eq}(\vec{r}, \vec{p})$ in the collision integral, leads to a significant enhancement of the damping of the nuclear giant multipole resonances. However, there is a conceptual disadvantage for the application of the Fermi distribution function $f_{eq,F}(\vec{r}, \vec{p})$ with $a(r) \neq 0$ to the collision integral. Namely, with this function the gain and loss terms in the collision integral are each nonzero for the ground state of the system, where the probability current should be absent by definition. We show in this work that in order to overcome this difficulty the smooth quantum distribution function $\tilde{f}_{eq}(\vec{r}, \vec{p})$ should be used for $f_{eq}(\vec{r}, \vec{p})$ in the collision integral in the kinetic Landau-Vlasov equation. In contrast to the Fermi distribution function $f_{eq,F}(\vec{r}, \vec{p})$, the smooth quantum distribution function $\tilde{f}_{eq}(\vec{r}, \vec{p})$ contains the residual oscillations [19,23] ensuring the above-mentioned condition for the disappearance of the gain and loss terms in the collision integral for the ground state and reducing the internal collisional width of the giant multipole resonances.

In this paper we pay attention mainly to finite size and memory effects in the relaxation processes in finite Fermi systems. In Sec.II we obtain a general expression for the width of the giant multipole resonances at zero temperature of the nucleus starting from the collisional Landau-Vlasov equation. In Sec. III we study the influence of the memory effects and the diffusivity of the Fermi surface on the relaxation time. We use the smeared-out Wigner distribution function $\tilde{f}_{eq}(\vec{r}, \vec{p})$ of the three-dimensional harmonic oscillator and of the Woods-Saxon potential for the calculations of the collision integral. A summary and conclusions are given in Sec. IV.

II. DAMPING OF COLLECTIVE EXCITATIONS IN KINETIC THEORY

The kinetic equation for a small variation $\delta f(\vec{r}, \vec{p}, t)$ of the distribution function can be transformed to a set (infinite) of equations for the moments of $\delta f(\vec{r}, \vec{p}, t)$ in \vec{p} space, namely, the local particle density $\delta\rho$, velocity field \vec{u} , pressure tensor $\pi_{\alpha\beta}$, etc., see [11,24]. The first-order moment of the kinetic equation has the form of the Euler-Navier-Stokes equation and is given by [24,25]

$$m\rho_{eq}\frac{\partial}{\partial t}u_\alpha + \rho_{eq}\frac{\partial}{\partial r_\nu}\left(\frac{\delta^2\mathcal{E}}{\delta\rho^2}\right)_{eq}\delta\rho + \frac{\partial}{\partial r_\nu}\pi_{\nu\alpha} = 0, \quad (3)$$

Here and in the following expressions, repeated greek indices $\alpha, \beta, \nu = 1, 2, 3$ are to be understood as summed over. The variation of the local particle density ρ and the velocity field u_α in Eq. (3) are defined by

$$\delta\rho = g \int \frac{d\vec{p}}{(2\pi\hbar)^3} \delta f, \quad \vec{u} = g \int \frac{d\vec{p}}{(2\pi\hbar)^3} \frac{\vec{p}}{m} \delta f. \quad (4)$$

The quantity $\pi_{\alpha\beta}$ is the deviation of the pressure tensor from its equilibrium part P_{eq} due to the Fermi-surface deformation

$$\pi_{\alpha\beta} = \frac{g}{m} \int \frac{d\vec{p}}{(2\pi\hbar)^3} (p_\alpha - mu_\alpha)(p_\beta - mu_\beta) \delta f \quad (5)$$

and the equilibrium pressure, P_{eq} , is given by

$$P_{eq} = g \int \frac{d\vec{p}}{(2\pi\hbar)^3} \frac{p^2}{2m} f_{eq} \equiv \frac{2}{3} \mathcal{E}_{kin}, \quad (6)$$

where \mathcal{E}_{kin} is the kinetic energy density. The internal energy density \mathcal{E} in Eq. (3) contains both kinetic and potential energy densities: $\mathcal{E} = \mathcal{E}_{kin} + \mathcal{E}_{pot}$, where \mathcal{E}_{pot} is the potential energy density.

Eq. (3) is not closed because it contains the pressure tensor $\pi_{\alpha\beta}$ given by the second-order moment of the distribution function $\delta f(\vec{r}, \vec{p}, t)$, Eq. (5). We will follow the nuclear fluid dynamic approach of Refs. [2,3,6] and take into account the dynamic Fermi-surface distortions up to multipolarity $l = 2$. The second \vec{p} moment of the kinetic equation leads then to a closed differential equation for the pressure tensor $\pi_{\alpha\beta}$. Namely (see Refs. [3,6,8,9,26]),

$$\frac{\partial}{\partial t}\pi_{\alpha\beta} + P_{eq}\left(\frac{\partial u_\alpha}{\partial r_\beta} + \frac{\partial u_\beta}{\partial r_\alpha} - \frac{2}{3}\delta_{\alpha\beta}\frac{\partial u_\alpha}{\partial r_\beta}\right) = -\frac{\pi_{\alpha\beta}}{\tau_2}. \quad (7)$$

The local relaxation time τ_2 in Eq. (7) is caused by the interparticle scattering on the deformed Fermi surface:

$$\frac{1}{\tau_2} = -\frac{\int d\vec{p}p^2 Y_{20} \delta St}{\int d\vec{p}p^2 Y_{20} \delta f}. \quad (8)$$

Here $\delta St \equiv \delta St(\vec{r}, \vec{p}, t)$ is a collision integral linearized in δf . In the case of small eigenibrations with eigenfrequency $\omega = \omega_0 + i\Gamma/2\hbar$, where ω_0 and Γ are real, the collision integral can be transformed, taking into account also memory effects, as [5,27]

$$\begin{aligned} \delta St(\vec{r}, \vec{p}, t) &= \int \frac{g d\vec{p}_2 d\vec{p}_3 d\vec{p}_4}{(2\pi\hbar)^6} \\ &\times W(\{\vec{p}_j\}) \sum_{j=1}^4 \frac{\delta Q}{\delta f_j} \Big|_{eq} \delta f_j \frac{1}{2} (\delta(\Delta E + \hbar\omega_0) + \delta(\Delta E - \hbar\omega_0)) \delta(\Delta\vec{p}), \end{aligned} \quad (9)$$

where $W(\{\vec{p}_j\})$ is the probability of the scattering of nucleons near the Fermi surface, $g = 4$ is the spin-isospin degeneracy factor and

$$Q = (1 - f_1)(1 - f_2)f_3f_4 - f_1f_2(1 - f_3)(1 - f_4);$$

$$\Delta E = E_1 + E_2 - E_3 - E_4; \quad \Delta\vec{p} = \vec{p}_1 + \vec{p}_2 - \vec{p}_3 - \vec{p}_4;$$

$E_j = p_j^2/2m + V(\vec{r}_j)$ is the classical single-particle energy, $\vec{p}_1 \equiv \vec{p}$ and $V(\vec{r})$ is the nuclear mean field.

We will follow the arguments of the Fermi-liquid theory of Ref. [24] and assume that the dynamical component of the distribution function $\delta f(\vec{r}, \vec{p}, t)$ has the form

$$\delta f(\vec{r}, \vec{p}, t) = -\frac{\partial f_{eq}}{\partial E} \nu(\vec{r}, \vec{p}, t), \quad (10)$$

where $\nu(\vec{r}, \vec{p}, t)$ are unknown functions. The functions $\nu(\vec{r}, \vec{p}, t)$ depend on the orientation \hat{p} only because of the sharp energy dependence of the factor $\partial f_{eq}/\partial E$ in Eq. (10), which is localized at the Fermi momentum $p_F(r)$. We point out that the smooth region of the equilibrium distribution function $f_{eq}(\vec{r}, \vec{p})$ in momentum space appears in a classical forbidden region at $E < V(\vec{r})$. However, this region is absent in the space integral in Eq. (9). Thus,

$$\nu(\vec{r}, \vec{p}, t) \approx \nu(\vec{r}, p_F(r), \hat{p}, t) = \sum_{lm} \nu_{lm}(\vec{r}, t) Y_{lm}(\hat{p}). \quad (11)$$

An exact evaluation of the nine-dimension integral in \vec{p} space in Eq. (9) is a very complicated problem. We will follow the Abrikosov-Khalatnikov method [24] improved in Ref. [28]. Let us assume that the scattering probability $W(\{\vec{p}_j\})$ in Eq. (9) depends on two scattering angles θ and ϕ only, (see Ref. [24]), where θ is the angle between \vec{p}_1 and \vec{p}_2 , and ϕ is the angle between the planes formed by (\vec{p}_1, \vec{p}_2) and (\vec{p}_3, \vec{p}_4) , i.e.,

$$W(\{\vec{p}_j\}) \approx W(\{p_j = p_F(r), \theta, \phi\}). \quad (12)$$

To evaluate the collision integral Eq. (9), we will use the Abrikosov-Khalatnikov transformation [24,28]:

$$\int \frac{d\vec{p}_2 d\vec{p}_3 d\vec{p}_4}{(2\pi\hbar)^6} \delta(\Delta\vec{p}) (\dots) \approx \frac{m^3}{2(2\pi\hbar)^6} \int \frac{d\Omega d\phi_2}{\cos\theta/2} dE_2 dE_3 dE_4 (\dots), \quad (13)$$

where $d\Omega = \sin\theta d\theta d\phi$ and ϕ_2 is the azimuthal angle of the momentum \vec{p}_2 in the coordinate system with the z axes along \vec{p}_1 . We point out that the angle ϕ varies only from 0 to π because the particles are indistinguishable.

Using Eq. (13), the collision integral Eq. (9) can be written in the form

$$\begin{aligned} \delta St(\vec{r}, \vec{p}, t) &= -\frac{m^3}{16\pi^4\hbar^6} \\ &\times \sum_{l,m} \nu_{lm}(\vec{r}, t) Y_{lm}(\hat{p}) \sum_{j=1}^4 \langle W(\theta, \phi) P_l(\cos\theta_j) \rangle (I_j^{(+)} + I_j^{(-)}). \end{aligned} \quad (14)$$

The symbol $\langle \dots \rangle$ denotes the averaging over angles of the relative momentum of the colliding particles

$$\langle W(\theta, \phi) P_l(\cos\theta_j) \rangle = \int_0^\pi d\theta \frac{\sin\theta}{\cos\theta/2} \int_0^\pi \frac{d\phi}{2\pi} W(\theta, \phi) P_l(\cos\theta_j), \quad (15)$$

where $\cos\theta_j \equiv (\hat{p}_j \hat{p}_1)$, i.e., $\theta_2 \equiv \theta$, and

$$\cos\theta_3 = (\cos(\theta/2))^2 + (\sin(\theta/2))^2 \cos\phi, \quad \cos\theta_4 = (\cos(\theta/2))^2 - (\sin(\theta/2))^2 \cos\phi,$$

$P_l(\cos\theta)$ is a Legendre polynomial and

$$I_j^{(\pm)} = \int_{V_{eq}}^\infty dE_2 dE_3 dE_4 \frac{\partial f_{eq,j}}{\partial E_j} \frac{\delta Q}{\delta f_j} \Big|_{eq} \delta(\Delta E \pm \hbar\omega_0).$$

We now return to the dynamical equation (3). Let us introduce the displacement field $\vec{\chi}(\vec{r}, t)$ related to the velocity field $\vec{u}(\vec{r}, t)$ as

$$\vec{u}(\vec{r}, t) = \frac{\partial}{\partial t} \vec{\chi}(\vec{r}, t). \quad (16)$$

We look for the displacement field $\vec{\chi}(\vec{r}, t)$ in the following separable form:

$$\vec{\chi}(\vec{r}, t) = \beta(t) \vec{v}(\vec{r}), \quad (17)$$

where $\beta(t) = \beta_0 e^{i\omega t}$. Substituting Eqs. (16) and (17) into Eq. (3), one obtains the equation of motion for the collective variable $\beta(t)$:

$$\begin{aligned} m\rho_{eq}v_\alpha\ddot{\beta} + \frac{1}{\omega} \frac{\partial}{\partial r_\nu} (\text{Im}\Pi_{\nu\alpha}^\omega) \dot{\beta} + \frac{\partial}{\partial r_\nu} (\text{Re}\Pi_{\nu\alpha}^\omega) \beta - \\ - \rho_{eq} \frac{\partial}{\partial r_\alpha} \left[\left(\frac{\delta^2 \mathcal{E}}{\delta \rho^2} \right)_{eq} \frac{\partial}{\partial r_\nu} (\rho_{eq} v_\nu) \right] \beta = 0, \end{aligned} \quad (18)$$

where we have used the following form for the traceless part $\pi_{\alpha\beta}(\vec{r}, t)$ of the momentum flux tensor

$$\pi_{\alpha\beta}(\vec{r}, t) \equiv \Pi_{\alpha\beta}^\omega(\vec{r}) \beta_0 e^{i\omega t} = \beta(t) \text{Re}\Pi_{\alpha\beta}^\omega(\vec{r}) + \frac{1}{\omega} \dot{\beta}(t) \text{Im}\Pi_{\alpha\beta}^\omega(\vec{r}). \quad (19)$$

Multiplying Eq. (18) by v_α , summing over α and integrating over \vec{r} space, we obtain the dispersion equation for the eigenfrequency ω :

$$-B\omega^2 + i\omega A(\omega) + \tilde{C}(\omega) = 0. \quad (20)$$

Here, B is the hydrodynamical mass coefficient [29] with respect to the collective variable $\beta(t)$:

$$B = m \int d\vec{r} \rho_{eq} v^2. \quad (21)$$

The dissipative term $A(\omega)$ and the stiffness coefficient $\tilde{C}(\omega) = C + C'(\omega)$ are given by

$$A(\omega) = \frac{1}{\omega} \int d\vec{r} v_\alpha \frac{\partial}{\partial r_\nu} (\text{Im}\Pi_{\nu\alpha}^\omega) \quad (22)$$

and

$$C = \int d\vec{r} \left(\frac{\delta^2 \mathcal{E}}{\delta \rho^2} \right)_{eq} \left[\frac{\partial}{\partial r_\nu} (\rho_{eq} v_\nu) \right]^2, \quad (23)$$

$$C'(\omega) = \int d\vec{r} v_\alpha \frac{\partial}{\partial r_\nu} (\text{Re} \Pi_{\nu\alpha}^\omega). \quad (24)$$

We point out that the definition of the stiffness coefficient C coincides with the one for the stiffness coefficient in the traditional liquid drop model (LDM) for the nucleus. In contrast, the additional contribution $C'(\omega)$ to the stiffness coefficient is absent in the LDM and represents the influence of the dynamical Fermi-surface distortion on the conservative forces in the Fermi system. Finally, the dissipative term $A(\omega)$ appears due to the interparticle scattering on the distorted Fermi surface.

To evaluate the coefficients $A(\omega)$ and $C'(\omega)$, we will use the third equation of motion (7). Let us rewrite Eq. (7) in the form

$$\frac{\partial}{\partial t} \pi_{\alpha\beta} + \frac{1}{\tau_2} \pi_{\alpha\beta} = -P_{eq} \Lambda_{\alpha\beta}, \quad (25)$$

where

$$\Lambda_{\alpha\beta} = \frac{\partial u_\alpha}{\partial r_\beta} + \frac{\partial u_\beta}{\partial r_\alpha} - \frac{2}{3} \delta_{\alpha\beta} \frac{\partial u_\alpha}{\partial r_\beta}. \quad (26)$$

Taking Eqs. (16), (19) and (25), one obtains

$$\dot{\beta} \text{Re} \Pi_{\alpha\beta}^\omega + \frac{1}{\omega} \ddot{\beta} \text{Im} \Pi_{\alpha\beta}^\omega + \frac{1}{\tau_2} \beta \text{Re} \Pi_{\alpha\beta}^\omega + \frac{1}{\omega \tau_2} \dot{\beta} \text{Im} \Pi_{\alpha\beta}^\omega = -P_{eq} \dot{\beta} \bar{\Lambda}_{\alpha\beta}. \quad (27)$$

Here,

$$\bar{\Lambda}_{\alpha\beta} = \frac{\partial v_\alpha}{\partial r_\beta} + \frac{\partial v_\beta}{\partial r_\alpha} - \frac{2}{3} \delta_{\alpha\beta} \frac{\partial v_\alpha}{\partial r_\beta}. \quad (28)$$

Eq. (27) can be represented as a set of equations of motion for both the real and the imaginary parts of ω :

$$-\Gamma \text{Re} \Pi_{\alpha\beta}^\omega - 2\hbar\omega_0 \text{Im} \Pi_{\alpha\beta}^\omega + \frac{2\hbar}{\tau_2} \text{Re} \Pi_{\alpha\beta}^\omega - \Gamma P_{eq} \bar{\Lambda}_{\alpha\beta} = 0, \quad (29)$$

$$2\hbar\omega_0 \text{Re} \Pi_{\alpha\beta}^\omega - \Gamma \text{Im} \Pi_{\alpha\beta}^\omega + \frac{2\hbar}{\tau_2} \text{Im} \Pi_{\alpha\beta}^\omega + 2\hbar\omega_0 P_{eq} \bar{\Lambda}_{\alpha\beta} = 0, \quad (30)$$

where $\text{Im}(\omega) \equiv \Gamma/(2\hbar)$.

In the case of small damped collective motion, we find from Eq. (27)

$$\text{Re}\Pi_{\alpha\beta}^{\omega} = -P_{eq} \frac{(\omega_0\tau_2)^2}{1 + (\omega_0\tau_2)^2} \bar{\Lambda}_{\alpha\beta}, \quad (31)$$

$$\text{Im}\Pi_{\alpha\beta}^{\omega} = -P_{eq} \frac{\omega_0\tau_2}{1 + (\omega_0\tau_2)^2} \bar{\Lambda}_{\alpha\beta}. \quad (32)$$

Finally, we have from Eqs. (22), (24), (31) and (32), (see also Ref. [26]),

$$A(\omega_0) = \int d\vec{r} P_{eq} \frac{\tau_2}{1 + (\omega_0\tau_2)^2} \bar{\Lambda}_{\alpha\nu} \frac{\partial v_{\alpha}}{\partial r_{\nu}}, \quad (33)$$

$$C'(\omega_0) = \int d\vec{r} P_{eq} \frac{(\omega_0\tau_2)^2}{1 + (\omega_0\tau_2)^2} \bar{\Lambda}_{\alpha\nu} \frac{\partial v_{\alpha}}{\partial r_{\nu}}. \quad (34)$$

In the same case of small damped collective motion, the dispersion equation (20) is transformed as

$$-B(\omega_0^2 + i\frac{\Gamma}{\hbar}\omega_0) + i\omega_0 A(\omega_0) + \tilde{C}(\omega_0) = 0. \quad (35)$$

Thus,

$$\omega_0^2 = \frac{\tilde{C}(\omega_0)}{B}, \quad \Gamma = \hbar \frac{A(\omega_0)}{B}. \quad (36)$$

Using Eqs. (36), (33) and (34) we obtain the width Γ as

$$\begin{aligned} \Gamma &= \hbar\omega_0 \frac{\omega_0 A(\omega_0)}{\tilde{C}(\omega_0)} \\ &= \hbar\omega_0 \frac{\int d\vec{r} P_{eq} \bar{\Lambda}_{\alpha\nu} (\partial v_{\alpha}/\partial r_{\nu}) \omega_0 \tau_2 / [1 + (\omega_0\tau_2)^2]}{C + \int d\vec{r} P_{eq} \bar{\Lambda}_{\alpha\nu} (\partial v_{\alpha}/\partial r_{\nu}) (\omega_0\tau_2)^2 / [1 + (\omega_0\tau_2)^2]}. \end{aligned} \quad (37)$$

In the case of an isoscalar giant quadrupole resonance (GQR) one can assume [3,4,17] that the displacement field $\vec{v}(\vec{r})$ is the irrotational one and is given by $\vec{v} = (-x, -y, 2z)$. We have then $\bar{\Lambda}_{\alpha\nu} \frac{\partial v_{\alpha}}{\partial r_{\nu}} = 8$. Furthermore, the LDM stiffness coefficient C gives a negligible contribution to the total value $\tilde{C}(\omega)$ [3,17] and Eq. (37) is transformed as

$$\Gamma \cong \hbar\omega_0 \frac{\int d\vec{r} P_{eq} \omega_0 \tau_2 / [1 + (\omega_0\tau_2)^2]}{\int d\vec{r} P_{eq} (\omega_0\tau_2)^2 / [1 + (\omega_0\tau_2)^2]}. \quad (38)$$

Finally, in the rare collision regime ($\omega_0\tau \gg 1$) Eq. (38) is reduced as

$$\Gamma_r \simeq \hbar \int d\vec{r} \frac{P_{eq}}{\tau_2} / \int d\vec{r} P_{eq}. \quad (39)$$

III. RESULTS OF NUMERICAL CALCULATIONS

To study the space distribution of the collective damping, we will introduce the local damping parameter $\xi(r, \omega_0)$ related to the width Γ :

$$\Gamma \equiv \int d\vec{r} \xi(r, \omega_0), \quad (40)$$

where (see Eq. (38))

$$\xi(r, \omega_0) = \frac{\hbar\omega_0 P_{eq} \omega_0 \tau_2 / [1 + (\omega_0 \tau_2)^2]}{\int d\vec{r} P_{eq} (\omega_0 \tau_2)^2 / [1 + (\omega_0 \tau_2)^2]}, \quad (41)$$

is always a positive quantity. The local relaxation time $\tau_2 \equiv \tau_2(r, \omega_0)$ can be obtained by substituting Eq. (14) into Eq. (8) and is given by

$$\frac{1}{\tau_2(r, \omega_0)} = -\frac{m^3}{16\pi^4 \hbar^6} \langle W(\theta, \phi) \rangle \frac{R^{(+)} + R^{(-)}}{\int_{V_{eq}}^{\infty} dE (E - V_{eq})^{3/2} \frac{\partial f_{eq}}{\partial E}} \equiv \gamma(r, \omega_0), \quad (42)$$

where

$$R^{(\pm)} = \int_{V_{eq}}^{\infty} dE_1 dE_2 dE_3 dE_4 (E_1 - V_{eq})^{3/2} \delta(\Delta E \pm \hbar\omega_0) \\ \times \left(\frac{\partial f_{eq,1}}{\partial E_1} \frac{\delta Q}{\delta f_{eq,1}} + c_2 \frac{\partial f_{eq,2}}{\partial E_2} \frac{\delta Q}{\delta f_{eq,2}} + (1 + c_2 - d_2) \frac{\partial f_{eq,3}}{\partial E_3} \frac{\delta Q}{\delta f_{eq,3}} \right), \quad (43)$$

and the coefficients c_2 and d_2 are given by

$$c_2 = \langle W P_2(\cos \theta) \rangle / \langle W \rangle, \quad d_2 = \langle 3 W \sin^4 \frac{\theta}{2} \sin^2 \phi \rangle / \langle W \rangle. \quad (44)$$

To evaluate the relaxation time (42), we will study, first of all, the collision integral $St_{eq}(\vec{r}, \vec{p})$ in the ground state of the system which is given by (see also Eq. (9))

$$St_{eq}(\vec{r}, \vec{p}) = \int \frac{g d\vec{p}_2 d\vec{p}_3 d\vec{p}_4}{(2\pi\hbar)^6} W(\{\vec{p}_j\}) Q|_{eq} \delta(\Delta E) \delta(\Delta \vec{p}). \quad (45)$$

We will introduce also the total gain and loss fluxes of the probability in the ground state. They are given, respectively, by

$$J_{eq,gain} = \int d\vec{r}_1 \frac{g d\vec{p}_1 d\vec{p}_2 d\vec{p}_3 d\vec{p}_4}{(2\pi\hbar)^9} W(\{\vec{p}_j\}) [1 - f_{eq,1}][1 - f_{eq,2}]f_{eq,3}f_{eq,4} \delta(\Delta E) \delta(\Delta\vec{p}), \quad (46)$$

and

$$J_{eq,loss} = \int d\vec{r}_1 \frac{g d\vec{p}_1 d\vec{p}_2 d\vec{p}_3 d\vec{p}_4}{(2\pi\hbar)^9} W(\{\vec{p}_j\}) [1 - f_{eq,3}][1 - f_{eq,4}]f_{eq,1}f_{eq,2} \delta(\Delta E) \delta(\Delta\vec{p}). \quad (47)$$

One can see from both definitions, Eqs. (46) and (47), that $J_{eq,gain} = J_{eq,loss}$ and $St_{eq}(\vec{r}, \vec{p}) = 0$, as it should be for the equilibrium state of system. Moreover, in the case of the ground state of the system, both fluxes $J_{eq,gain}$ and $J_{eq,loss}$ have to disappear separately. This is not the case, however, if the Fermi distribution function $f_{eq,F}$ (see Eq. (2)) is used for the equilibrium distribution function f_{eq} of the ground state of the finite Fermi system in Eqs. (46) and (47). To avoid this disadvantage we will use the smeared-out quantum distribution function \tilde{f}_{eq} in both Eqs. (46) and (47). To control the disappearance of the gain and loss fluxes, we will introduce the relative contribution q of the probability fluxes $J_{eq,gain}$ or $J_{eq,loss}$ evaluated with $f_{eq} = \tilde{f}_{eq}$ to the corresponding values evaluated with $f_{eq} = f_{eq,F}$, i.e.,

$$q = J_{eq,gain}(\{\tilde{f}_{eq}\})/J_{eq,gain}(\{f_{eq,F}\}) \equiv J_{eq,loss}(\{\tilde{f}_{eq}\})/J_{eq,loss}(\{f_{eq,F}\}). \quad (48)$$

Below we will apply our approach to the isoscalar GQR. We will assume that the scattering probability W in Eqs. (42) and (44) is angle independent, i.e., $d_2 = 4/5$ and $c_2 = 1/5$, and the magnitude of W can be obtained from the nuclear matter estimate of the parameter $\alpha \equiv 15 \pi^2 \hbar^5/m^3 \langle W \rangle = 9.2 \text{ MeV}$ from Ref. [8]. We will also use the following expression for the energy $\hbar\omega_0$ of the isoscalar GQR, $\hbar\omega_0 = 60A^{-1/3} \text{ MeV}$. The numerical calculations will be performed for both the spherical harmonic oscillator (HO) potential well and the Woods-Saxon (WS) potential.

A. Spherical harmonic oscillator potential

We will use the harmonic oscillator potential in the form

$$V_{eq}(r) = \frac{1}{2}m\Omega^2 r^2, \quad (49)$$

where $\hbar\Omega \simeq 41A^{-1/3}$ MeV. For "magic" nuclei in the absence of the spin-orbit interaction, the smeared-out quantum distribution function $\tilde{f}_{eq}(\vec{r}, \vec{p})$ in a HO potential is given by [19]

$$\tilde{f}_{eq}(\vec{r}, \vec{p}) \equiv \tilde{f}_{eq}(\epsilon) = 8e^{-\epsilon} \sum_{k=0}^{\infty} (-1)^k L_k^2(2\epsilon) \tilde{n}_k. \quad (50)$$

Here, $L_k^n(\epsilon)$ is the associated Laguerre polynomial and $\epsilon = p^2/m\hbar\Omega + m\Omega r^2/\hbar \equiv 2E/\hbar\Omega$ is the dimensionless energy parameter. The smooth occupation numbers \tilde{n}_k are introduced as

$$\tilde{n}_k = \int_{-\infty}^{\tilde{\lambda}_k} dx \zeta(x) + \sum_{\mu=1}^M a_{2\mu} \zeta_{2\mu-1}(\tilde{\lambda}_k), \quad (51)$$

where $\zeta(x)$ is the averaging function chosen as

$$\zeta(x) = \frac{1}{\sqrt{\pi}} e^{-x^2}.$$

The second term in Eq. (51) contains the so-called Strutinsky curvature corrections and is given by

$$\zeta_n(x) = \frac{(-1)^n}{\sqrt{\pi}} e^{-x^2} H_n(x),$$

where $H_n(x)$ are the Hermite polynomials, $a_{2n} = (-1)^n/(2^{2n}n!)$, and $\tilde{\lambda}_k = (E_F - E_k)/\gamma$. The quantities E_F and E_k are the Fermi energy and single-particle energies in the mean field $V_{eq}(r)$, respectively, and γ is an averaging parameter.

The results of numerical calculations (see also Ref. [19]) of the smooth distribution function $\tilde{f}_{eq}(\epsilon)$ of Eq. (50) are shown in Fig. 1. The solid line 1 gives the behaviour of the smooth distribution function for the value of the smearing parameter $\gamma = 2.5 \cdot \hbar\Omega$ and $2M = 6$, the order of the curvature correction polynomial in Eq. (51). We point out that these values of the smearing parameter and correction polynomial are localized in the so-called plateau region for the shell correction δU to the binding energy, i.e., where δU does not depend on γ , Ref. [30].

The smooth distribution function $\tilde{f}_{eq}(\epsilon)$ exhibits oscillations caused by particle reflections on the potential surface. The mean behaviour (i.e., without the oscillations) of $\tilde{f}_{eq}(\epsilon)$ can

be approximated by the Fermi function $f_{eq,F}(\vec{r}, \vec{p})$ of Eq. (2), where the chemical potential λ is fixed by the condition of conservation of particle number A:

$$A = g \int \frac{d\vec{r}d\vec{p}}{(2\pi\hbar)^3} f_{eq,F}(\vec{r}, \vec{p}).$$

The solid line 2 in Fig. 1 shows the behaviour of the Fermi distribution function $f_{eq,F}(\vec{r}, \vec{p})$ of Eq. (2) with the parameter a taken from Eq. (55). The dashed line in Fig. 1 gives the simple Thomas-Fermi approximation Eq. (1).

In Fig. 2 we show the smooth distribution functions \tilde{f}_{eq} as functions of the dimensionless kinetic energy $\epsilon_{kin} = p^2/m\hbar\Omega$ for different distances r . We can see from this figure that the diffusivity parameter a is almost independent of the distance r . This fact is a feature of the HO potential well. Note that the analogous diffusivity parameter for the Woods-Saxon potential is a strongly r -dependent function increasing near the potential wall, see below and Ref. [22,23]. Following Ref. [23], the diffusivity parameter a of the quantum distribution function f_{eq} in momentum space can be estimated using the expansion of f_{eq} in Hermite polynomials. The result reads

$$a \simeq \sqrt{G_2 + \left[\frac{G_3}{2}\right]^{2/3}}. \quad (52)$$

The parameters G_2 and G_3 depend on the mean field $V(r)$ and are given by (in the lowest order of \hbar^2)

$$G_2 = -\frac{\hbar^2}{4m} \left[\frac{2}{r} V'_{eq}(r) + V''_{eq}(r) \right], \quad G_3 = -\frac{\hbar^2}{4m} \left[(V'_{eq}(r))^2 + \frac{p^2}{3m} \left[\frac{2}{r} V'_{eq}(r) + V''_{eq}(r) \right] \right], \quad (53)$$

where *prime* means an r derivative. For the HO potential one has $G_2 = -3(\hbar\Omega)^2/4$ and $G_3 \simeq -(\hbar\Omega)^3\lambda/2$. The diffusivity parameter a can be also estimated from a fit of the smooth distribution function \tilde{f}_{eq} and its derivative $d\tilde{f}_{eq}/dE$ to the corresponding values of the Fermi distribution function Eq. (2) within some smeared out interval $\tilde{\gamma} \leq \gamma$ near the Fermi energy E_F . Namely, one has the following estimate:

$$a = \frac{1}{\tilde{\gamma}} \int_{E_F - \tilde{\gamma}/2}^{E_F + \tilde{\gamma}/2} dE \frac{\tilde{f}_{eq}(\tilde{f}_{eq} - 1)}{d\tilde{f}_{eq}/dE}. \quad (54)$$

Note that Eq. (54) gives an exact result for the diffusivity parameter a if the distribution function \tilde{f}_{eq} coincides with the Fermi distribution function of Eq. (2).

The solid lines 1 and 2 in Fig. 3 show the numerical results for the parameter a as a function of mass number A obtained using both expressions (52) and (54), respectively. A discrepancy between the results presented by curves 1 and 2 appears because the expression (52) takes into account the lowest orders of expansion of the distribution function \tilde{f}_{eq} over the Hermite polynomials; see Ref. [23]. We have also established the following simple A dependence for the diffusivity parameter a for the spherical HO potential well, obtained from Eq. (54) with $\tilde{\gamma} = \gamma/2 = 1.25 \hbar\Omega$,

$$a \approx 10.2A^{-1/6} \text{ MeV}. \quad (55)$$

The result of the numerical calculation of the diffusivity parameter a Eq. (55) is shown in Fig. 3 by the dashed line.

We will return now to the problem of evaluating the relaxation time, Eq. (8). In Fig. 4 we have plotted the ratio q as obtained from Eq. (48) as a function of the mass number A (curve HO for the harmonic oscillator potential (49)). We have used here the Fermi distribution function Eq. (2) with parameter a from Eq. (55). As can be seen from Fig. 4, the effect of the quantum oscillations for the smeared-out distribution function $f_{eq} = \tilde{f}_{eq}$ leads to an essential compensation of the gain and loss probability fluxes. A small nonzero contribution (about 10 - 20 % in Fig. 4) remains in part because of the Abrikosov-Khalatnikov transformation Eq. (13) used earlier, which implies a localization of the momentum \vec{p}_j near the Fermi surface in Eq. (9). In order to check this statement, we will use more general transformation of the momentum integrals in the collision integral, Eq. (9), with an arbitrary value of the momentum p_j , suggested in Ref. [7]:

$$\begin{aligned} & \int \frac{d\vec{p}_2 d\vec{p}_3 d\vec{p}_4}{(2\pi\hbar)^6} \delta(\Delta\vec{p}) \delta(\Delta E) (\dots) \\ &= \frac{m^3}{16\pi^4 \hbar^4 p_1} \int dE_2 dE_3 \left[\sqrt{p_1^2 + p_2^2 + 2p_1 p_2 \kappa} - \sqrt{p_1^2 + p_2^2 - 2p_1 p_2 \kappa} \right] (\dots), \end{aligned} \quad (56)$$

where $\kappa = \min\left(1, \sqrt{p_3^2(p_1^2 + p_2^2 - p_3^2)/p_1^2 p_2^2}\right)$. The solid line 1 in Fig. 5 gives the behaviour

of the ratio q as a function of the smoothing parameter γ as obtained from Eq. (48) by applying the transformation Eq. (56) to the calculations of the probability fluxes, Eqs. (46) and (47). A strong deviation of this result for q from the analogous one obtained using the Abrikosov-Khalatnikov procedure, Eq. (13), (the solid line 2) appears for small magnitudes of smoothing parameter γ . This is because the smeared-out distribution function \tilde{f}_{eq} oscillations grow with the decrease of the smoothing parameter γ and the accuracy of the Abrikosov-Khalatnikov transformation Eq. (13) also decreases.

The results of the numerical calculations of the local relaxation time (more precisely, the inverse value $\hbar/\tau_2(r, \omega_0)$) of Eq. (42) for the isoscalar GQR in the nucleus with $A = 224$ are shown in Fig. 6. We point out that the use of the Fermi distribution function Eq. (2) instead of \tilde{f}_{eq} in Eq. (42) (the solid curve 2 in Fig. 6) leads to much stronger damping than the analogous calculations with \tilde{f}_{eq} from Eq. (50) (solid curve 1).

To give a simple phenomenological prescription for the removal of the nonphysical probability fluxes (46) and (47) in the ground state of a system, we will introduce the modified distribution function

$$\mathcal{F}_{eq} = f_{eq,F} + \eta \Delta \tilde{f}_{eq}. \quad (57)$$

Here, $f_{eq,F}$ is the Fermi distribution function Eq. (2) with diffusivity parameter a from Eq. (55), and $\Delta \tilde{f}_{eq}$ is given by

$$\Delta \tilde{f}_{eq} = \tilde{f}_{eq} - f_{eq,F},$$

where \tilde{f}_{eq} is the smooth distribution function of Eq. (50). A numerical calculation of the probability fluxes $J_{eq,gain}$, Eq. (46), and $J_{eq,loss}$, Eq. (47), with \tilde{f}_{eq} replaced by \mathcal{F}_{eq} shows that both probability fluxes disappear at $\eta = 0.86$ for the nucleus with $A = 224$. The corresponding distribution function \mathcal{F}_{eq} is shown in Fig. 1 as the dotted line. The local relaxation time from Eq. (42) obtained with modified distribution function from Eq. (57) is shown in Fig. 6 as solid curve 3. It should be remembered that the two last results (curves 1 and 3) are more correct in the sense of the compensation of the probability fluxes in the ground state of the system. Both these results show strong oscillations of the local

relaxation time within the nuclear volume and amplification of the damping in the surface region of the nucleus. This feature of the finite Fermi system arises due to the fact that the equilibrium distribution function \tilde{f}_{eq} , Eq. (50) fluctuates strongly and contains the diffusivity of the Fermi surface. It is interesting to note that, excluding the oscillations in the nuclear volume, the result noted as curve 3 in Fig. 6 with full compensation of the probability fluxes in the ground state is in good agreement with the one $(\hbar/\tau_2)_{TF}$ obtained using the simple Thomas-Fermi distribution function of Eq. (1) (the dashed line in Fig. 6 with $(\hbar/\tau_2)_{TF} = 3(\hbar\omega_0)^2/(4\pi^2\alpha)$).

We point out that the quantum calculations represented in Fig. 6 by curves 1 and 3 have been done with a quite large smoothing parameter $\gamma = 2.5 \cdot \hbar\Omega$. A decrease of γ leads to negative values of the local relaxation time $\tau_2(r, \omega_0)$ in some regions of r . The behaviour of the damping factor $\xi(r, \omega_0)$ is shown in Fig. 7. It is necessary to stress that nonzero damping in a cold Fermi system appears only because of the memory effects in the collision integral (9).

The results of numerical calculations of the width Γ of the isoscalar GQR as a function of the mass number A are shown in Fig. 8. As can be seen from this figure, the smooth distribution function \tilde{f}_{eq} from Eq. (50) leads to the contribution of the collisional relaxation to the isoscalar GQR width (solid line 1) which does not exceed 30-50% of the experimental values. This result is similar to the one obtained with the sharp Thomas-Fermi distribution function Eq. (1) (the dashed line) and agrees with the earlier calculation of the internal collisional width of the isoscalar GQR [6]. In contrast, the analogous calculation with the smooth Fermi distribution function (2) (solid line 2) largely overestimates the contribution of collisional damping. Note that the small nonzero probability fluxes appearing in $J_{eq,gain}$ (46) and $J_{eq,loss}$ (47) evaluated with \tilde{f}_{eq} from Eq. (50) lead to a very small contribution to the final result for the width. This can be seen in Fig. 8 from a comparison of both curves 1 and 3.

B. Woods-Saxon potential

We have applied above the HO Wigner distribution function to the calculations of the collision integral in a finite Fermi system. This distribution function contains both important ingredients of influence of the multiple particle reflections from the potential surface: the diffusivity and the oscillations of the distribution function in momentum space. However, the realistic nuclear potential well has a finite depth, providing stronger surface effects than the ones in the HO mean field. We will give below an analysis for the case of the WS potential in the form

$$V_{WS}(r) = V_0/(1 + \exp[(r - R_0)/d]). \quad (58)$$

We have adopted the following parameters $V_0 = -44 \text{ MeV}$ $R_0 = 1.27 \text{ A}^{1/3}$ and $d = 0.67 \text{ fm}$.

An exact quantum calculation of the equilibrium distribution function $f_{eq}(\vec{r}, \vec{p})$ for the WS potential is a rather complicated problem. We will use the result of Ref. [23] for the semiclassical expansion of $f_{eq}(\vec{r}, \vec{p})$ in the Hermite polynomials. This gives

$$f_{eq}(\vec{r}, \vec{p}) = \sum_{n=0}^N \frac{b_n (-1)^n}{n!} \Phi^{(n)}\left(\frac{x - \mu}{\sigma}\right) \Big|_{x=E_F}. \quad (59)$$

Here $\Phi(y) = [1 + \text{erf}(y/\sqrt{2})]/2$ is the normal distribution function, $\text{erf}(y)$ is the error function, $\Phi^{(0)} \equiv \Phi$ and the index n at $\Phi^{(n)}((x - \mu)/\sigma)$ denotes the x derivative of n order. We will take into account terms with $n \leq 3$ in the expansion (59). The corresponding coefficients b_n are given by

$$b_0 = 1; \quad b_1 = E(\vec{r}, \vec{p}) - \mu; \quad b_2 = G_2 + b_1^2 - \sigma^2; \quad b_3 = G_3 + b_1^3 + 3b_1(G_2 - \sigma^2),$$

where G_2 and G_3 are obtained from (53). The coefficients μ and σ can be found by solving the following nonlinear equations:

$$b_4 \equiv b_1^4 + 6b_1^2(G_2 - \sigma^2) + 4b_1G_3 + 3\sigma^2(\sigma^2 - 2G_2) = 0,$$

$$b_5 \equiv 15\sigma^4b_1 - 10\sigma^2(b_1^3 + 3b_1G_2 + G_3) - b_1^5 - 10b_1^3G_2 - 10b_1^2G_3 = 0.$$

Following Eq. (2), the mean behaviour of $f_{eq}(\vec{r}, \vec{p})$, Eq. (59), can be approximated by the following Fermi function:

$$f_{eq,WS}(\vec{r}, \vec{p}) = \left(1 + \exp \left[\frac{E(\vec{r}, \vec{p}) - \lambda}{a(r)} \right] \right)^{-1}. \quad (60)$$

Here $E(\vec{r}, \vec{p})$ is the classical energy of the particle in the WS potential

$$E(\vec{r}, \vec{p}) = \frac{p^2}{2m} + V_{WS}(r).$$

The local diffusivity $a(r)$ is evaluated from Eq. (53) with G_j taken in the so-called surface approximation ($V''_{eq}(r) \approx V''_{eq}(R_0) = 0$) [9]

$$G_2 = -\frac{\hbar^2}{4m} \left[\frac{2}{R_0} V'_{eq}(r) \right]; \quad G_3 = -\frac{\hbar^2}{4m} \left[(V'_{eq})^2 + \frac{p_F^2}{3m} \left[\frac{2}{R_0} V'_{eq}(r) \right] \right],$$

where $p_F(r) = \hbar(3\pi^2\rho_{eq}(r)/2)^{1/3}$ is the Fermi momentum taken in the local density approximation. The results of numerical calculations of the parameter $a(r)$ are plotted in Fig. 9 for both HO and WS distribution functions. We can see that the parameter $a(r)$ for the WS potential well is peaked in the vicinity of the nuclear surface. The distribution function $f_{eq}(\vec{r}, \vec{p})$ smeared out over angles in \vec{p} space is plotted in Fig. 10. It contains both diffusivity and oscillations in \vec{p} space which depend on the distance r . In Fig. 4 we show the ratio q as defined by Eq. (48) (curve WS). We have used there the Fermi distribution function, Eq. (60), instead of the smooth distribution function $f_{eq,F}$ in Eq. (48). One can see that the occurrence of the quantum oscillations in the smeared-out distribution function \tilde{f}_{eq} leads to an essential compensation of the gain and loss probability fluxes.

The local relaxation parameter (42) and the damping factor (41) are shown in Figs. 11 and 12, respectively. It can be seen that the collisional damping is more pronounced in the case of the WS potential than in the HO one shown in Figs. 6 and 7. We point out also that the occurrence of the quantum oscillations in the equilibrium distribution function strongly reduces the relaxation processes in the finite Fermi system. The total collisional width Γ of the isoscalar GQR as a function of the mass number A evaluated for WS potential is shown in Fig. 13. The final result (solid line 1) agrees with above calculation of the collisional width in the HO potential; see the dashed line in Fig. 8.

IV. SUMMARY AND CONCLUSIONS

Starting from the collisional kinetic equation we have derived the isoscalar GQR width for a finite nucleus taking into account the memory effects and the peculiarities of the equilibrium distribution function f_{eq} caused by the multiple reflections of particles on the potential wall. The equilibrium distribution function contains both smooth and the oscillating components. The smooth component of f_{eq} can be approximated by the Fermi distribution (2) with an r -dependent diffusivity parameter $a(r)$ in momentum space. The diffusivity parameter $a(r)$ is almost independent of the distance r in the case of the harmonic oscillator potential well and is a strongly r -dependent function in the case of the Woods-Saxon potential, increasing near the potential wall. We have demonstrated numerically that the smooth part of the equilibrium distribution function can be satisfactorily described by using the semiclassical expansion of $f_{eq}(\vec{r}, \vec{p})$ on the Hermite polynomials; see Ref. [23].

It was shown that the general condition for the disappearance of the gain and loss probability fluxes in the ground state of system can be reached due to the occurrence of quantum oscillations in the distribution function in momentum space in the nuclear volume. The diffuse tail of the distribution function in momentum space leads to an increase of the collisional damping of the collective motion in the surface region of the nucleus and thus to an increase of the isoscalar GQR width. However this increase is strongly reduced due to the above-mentioned oscillations of the equilibrium distribution functions appearing in the collision integral Eq. (9). As a result the collisional width of the isoscalar GQR does not exceed 30-50% of the experimental value and agrees with the estimates of the width where the sharp Thomas-Fermi distribution function (i.e., in the absence of the diffusivity and quantum oscillations) is used. The collisional damping in a cold Fermi system arises only because of memory effects in the collision integral (9).

To describe the experimental values of the multipole giant resonances additional contributions from other spreading sources, such as the fragmentation width in random phase approximation calculations or its representation through the one-body dissipation (see Ref.

[8]) have to be taken into account. We pointed out also that surface effects in the collisional damping are manifested more distinctly in the Woods-Saxon potential where the diffusivity parameter $a(r)$ of the distribution function in momentum space is r dependent and increases within the surface region of the nucleus.

ACKNOWLEDGEMENTS

This work was supported in part by the U.S. National Science Foundation under Grant No. PHY-9413872 and the INTAS under Grant No. 93-0151. We are grateful for this financial support. One of us (V.M.K.) thanks Professor P.Schuck for stimulating discussion and the Cyclotron Institute at Texas A&M University for the kind hospitality.

REFERENCES

- [1] G.B.Bertsch, Z. Phys. **A 289**, 103 (1978).
- [2] J.R.Nix and A.J.Sierk, Phys. Rev. C **21**, 199 (1980).
- [3] V.M. Kolomietz, *Local Density Approach for Atomic and Nuclear Physics* (Naukova Dumka, Kiev, 1990).
- [4] M. Di Toro, Sov. J. Part. Nucl. **22**, 185 (1991).
- [5] V.M.Kolomietz, A.G.Magner and V.A.Plujko, Z. Phys. A **345**, 131 (1993).
- [6] V.M.Kolomietz, V.A.Plujko and S.Shlomo, Phys. Rev. C **52**, 2480 (1995).
- [7] K.Sato and S.Yoshida, Phys. Rev. C **52**, 837 (1995).
- [8] V.M.Kolomietz, V.A.Plujko and S.Shlomo, Phys. Rev. C **54**, 3014 (1996).
- [9] V.M. Kolomietz, S.V.Lukyanov and V.A. Plujko, Izv. Ross. Akad. Nauk. Ser. Fiz. **61**, 121 (1997).
- [10] L.D.Landau, Sov. Phys. JETP **5**, 101 (1957).
- [11] E.M.Lifschitz and L.P.Pitajevsky, *Physical Kinetics* (Pergamon Press, Oxford, 1981).
- [12] E.P. Wigner, Phys. Rhev. **40**, 749 (1932).
- [13] S. Shlomo, Nuovo Cimento **A 87**, 211 (1985).
- [14] P. Carruthers and F. Zachariasen, Rev. Mod. Phys. **55**, 245 (1983).
- [15] S. Shlomo, Phys. Lett. **118B**, 233 (1982).
- [16] S. Shlomo, J. Phys. G **10**, (1179).
- [17] P. Ring and P. Schuck, *The Nuclear Many-Body Problem* (Springer-Verlag, New-York, 1980).
- [18] S. Shlomo and M. Prakash, Nucl. Phys. **A357**, 157 (1981).

- [19] M. Prakash, S. Shlomo and V.M. Kolomietz, Nucl.Phys. **A370**, 30 (1981).
- [20] M. Prakash, S. Shlomo, B.S. Nilsson, J.P. Bondorf, and F. Serr, Nucl. Phys. **A385**, 483 (1982).
- [21] M.V. Zverev and E.E. Sapershtein, Yad. Fiz. **43**, 304 (1986). [Sov. J. Nucl. Phys. **43**, 195 (1986)]
- [22] M.Durand, V.S.Ramamurthy and P.Schuck, Phys.Lett. **B113**, 116 (1982).
- [23] V.M. Kolomietz and V.A. Plujko, Physics of Atomic Nuclei **57**, 354 (1994).
- [24] A.A. Abrikosov and I.M. Khalatnikov, Rep. Prog. Phys. **22**, 329 (1959).
- [25] V.M.Kolomietz and H.H.K.Tang, Phys. Scripta **24**, 915 (1981).
- [26] D.Kiderlen, V.M.Kolomietz and S.Shlomo, Nucl.Phys. **A608**, 32 (1996).
- [27] V.M. Kolomietz and V.A. Plujko, Physics of Atomic Nuclei **57**, 931 (1994).
- [28] J. Vogel, E. Vogel and C. Toepffer, Ann. of Phys. **164**, 463 (1985).
- [29] A. Bohr and B.R. Mottelson, *Nuclear Structure*, Vol. 2 (Benjamin, New York, 1975).
- [30] V.M. Kolomietz, B.D. Konstantinov, V.M. Strutinsky and V.I. Khvorostyanov, Fiz. Elem. Chastits At. Yadra **3**, 392 (1972).
- [31] F.E. Bertrand, Nucl.Phys. **A354**, 129c (1981).
- [32] A. van der Woude, In: *Electric and Magnetic Giant Resonances in Nuclei*, edited by J. Speth. (Word Scientific, Singapore 1991), Chap. II, p.99.

FIGURES

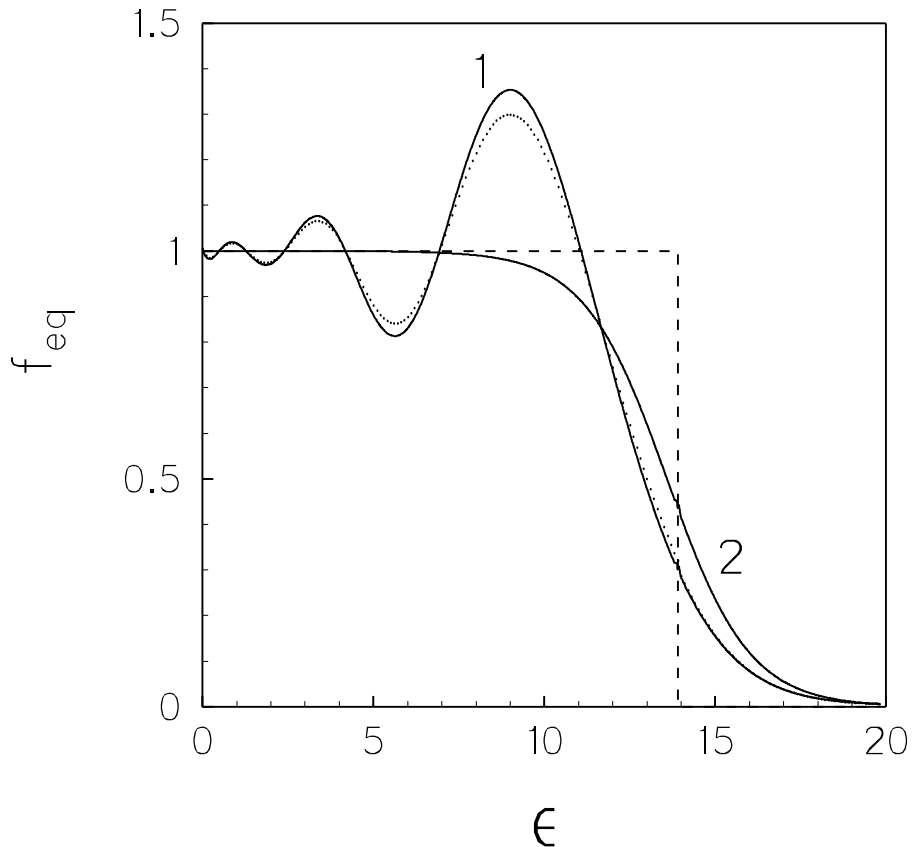


FIG. 1. The equilibrium distribution function as a function of the dimensionless parameter ϵ , for a nucleus with mass number $A= 224$, calculated for a spherical HO potential. Solid lines 1 and 2 show the smooth distribution function obtained using an averaging procedure of Eq. (50) with $\gamma = 2.5 \cdot \hbar\Omega$ and the Fermi distribution function of Eq. (2) with parameter a from Eq. (55), respectively. The dashed line shows the Thomas-Fermi distribution function (1). The dotted line shows the distribution function of Eq. (57) with $\eta = 0.86$ providing the disappearance of the probability fluxes in the ground state of the nucleus.

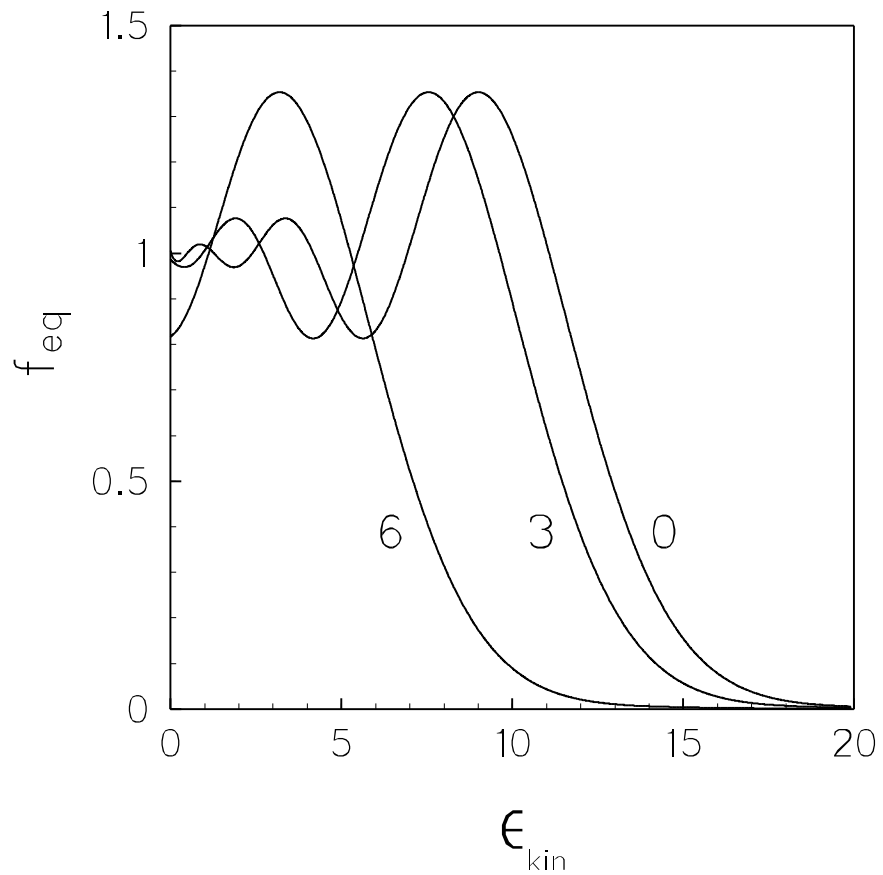


FIG. 2. The smooth distribution function of Eq. (50) as a function of the dimensionless kinetic energy $\epsilon_{kin} = p^2/m\hbar\Omega$, for a nucleus with mass number $A= 224$, calculated for a spherical HO potential with $\gamma = 2.5 \cdot \hbar\Omega$. The different curves correspond to the distances $r = 0, 3$, and $6 fm$ to the center of the nucleus.

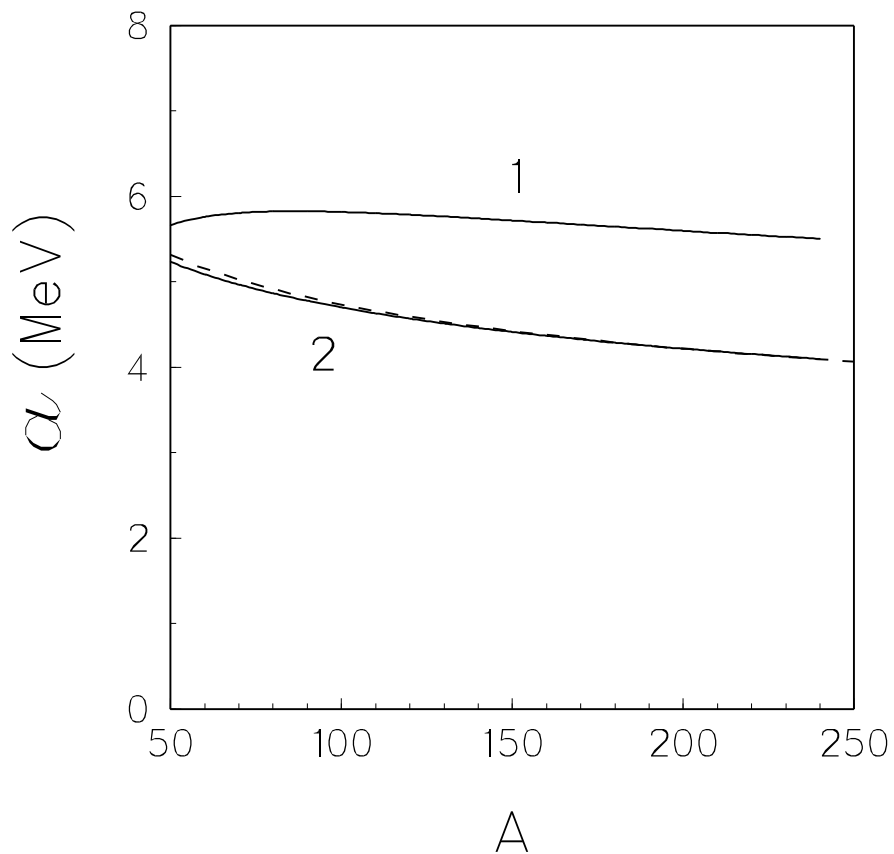


FIG. 3. The diffusivity parameter of the smooth distribution function of Eq. (50) versus the mass number A , calculated for a spherical HO potential with $\gamma = 2.5 \cdot \hbar\Omega$: For curve 1 we use Eq. (52), for curve 2 we use Eq. (54) and the dashed curve is obtained from the fitting formula of Eq. (55).

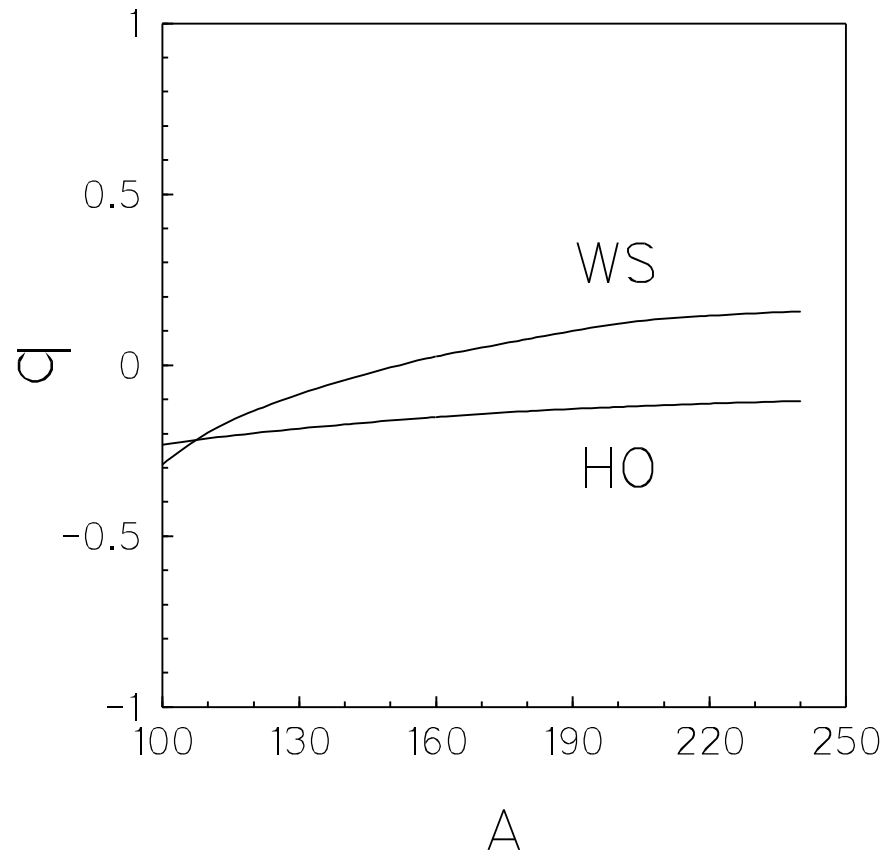


FIG. 4. The relative probability fluxes as given by Eq. (48) versus the mass number A for both HO and WS potentials.

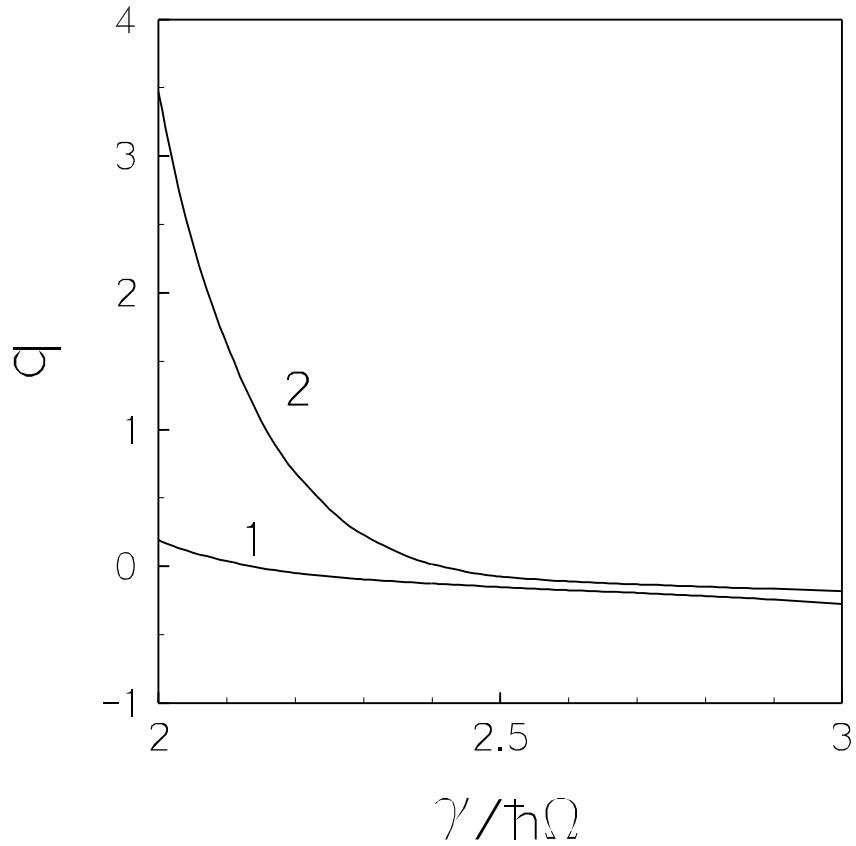


FIG. 5. Dependence of the relative probability fluxes q on the averaging parameter γ in units of $\hbar\Omega$: For solid line 2 we use the Abrikosov-Khalatnikov transformation Eq. (13), and for solid line 1 we use the transformation Eq. (56), for the momentum integrals in the collision integral Eq. (9). The calculations were performed for the nucleus with $A=224$ in the HO potential well.

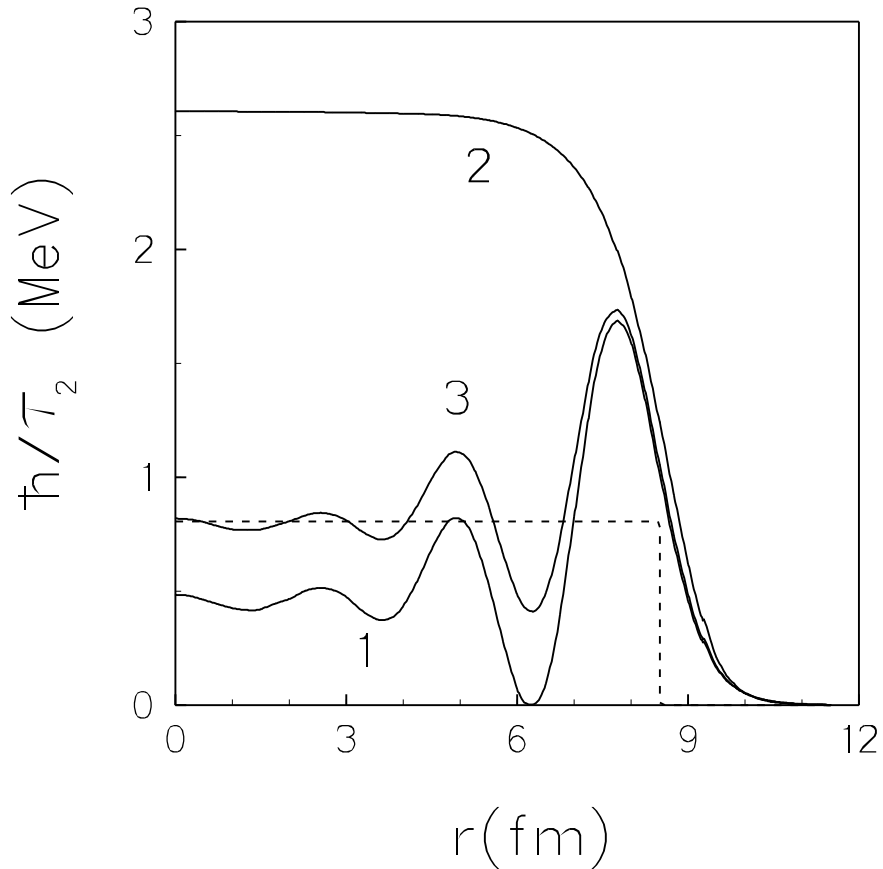


FIG. 6. The local damping parameter $\hbar/\tau_2(r, \omega_0)$ for the nucleus with $A = 224$, calculated for a spherical HO potential. The different curves correspond to the different equilibrium distribution function in Eq. (42): For curve 1 we use the smooth distribution function of Eq. (50) with averaging parameter $\gamma = 2.5 \cdot \hbar\Omega$, for curve 2 we use the Fermi distribution function (2) with a from Eq. (55), and for curve 3 we use the distribution function from Eq. (57). The dashed line shows the result obtained using the Thomas-Fermi distribution function of Eq. (1).

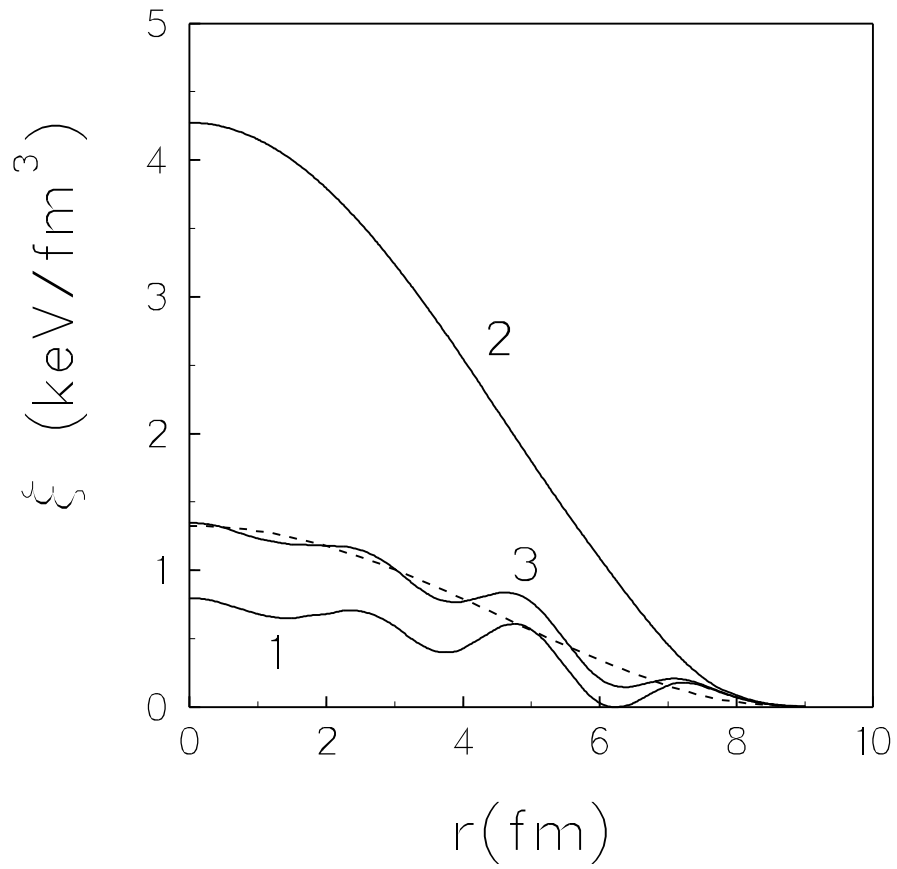


FIG. 7. The damping factor $\xi(r, \omega_0)$ as a function of the distance r . The notations is the same as in Fig. 6.

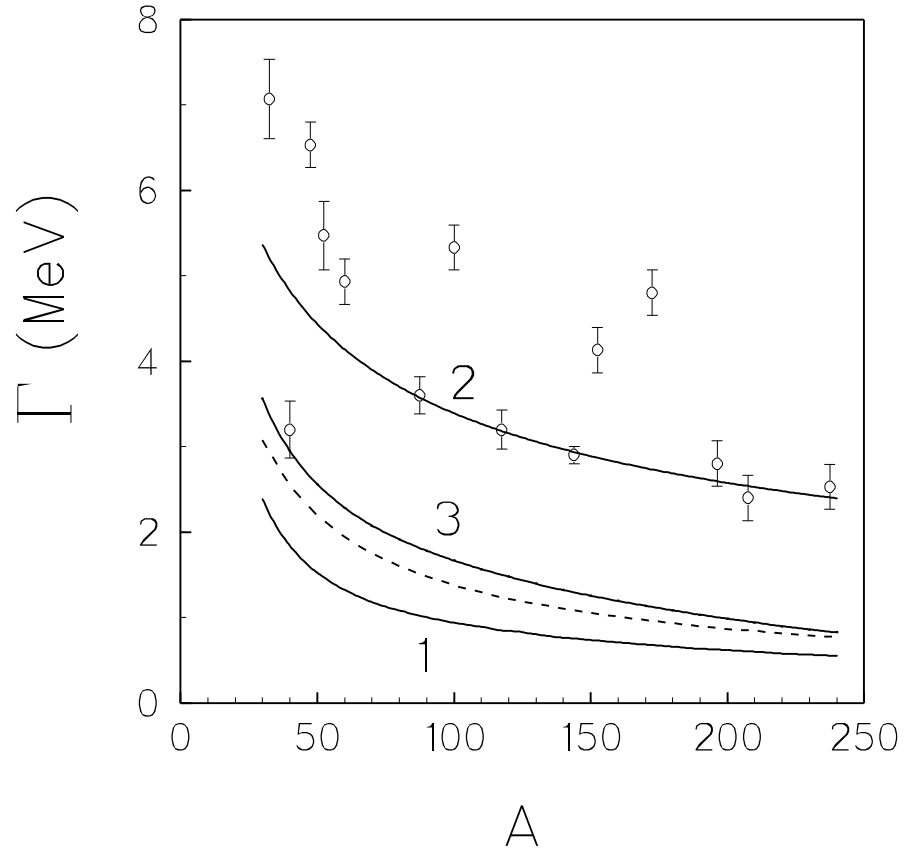


FIG. 8. The collisional width of the isoscalar giant quadrupole resonances obtained by using Eq. (40) with $\xi(r, \omega_0)$ from Fig. 7. The notations is the same as in Fig. 7. The experimental data were taken from Refs. [31, 32].

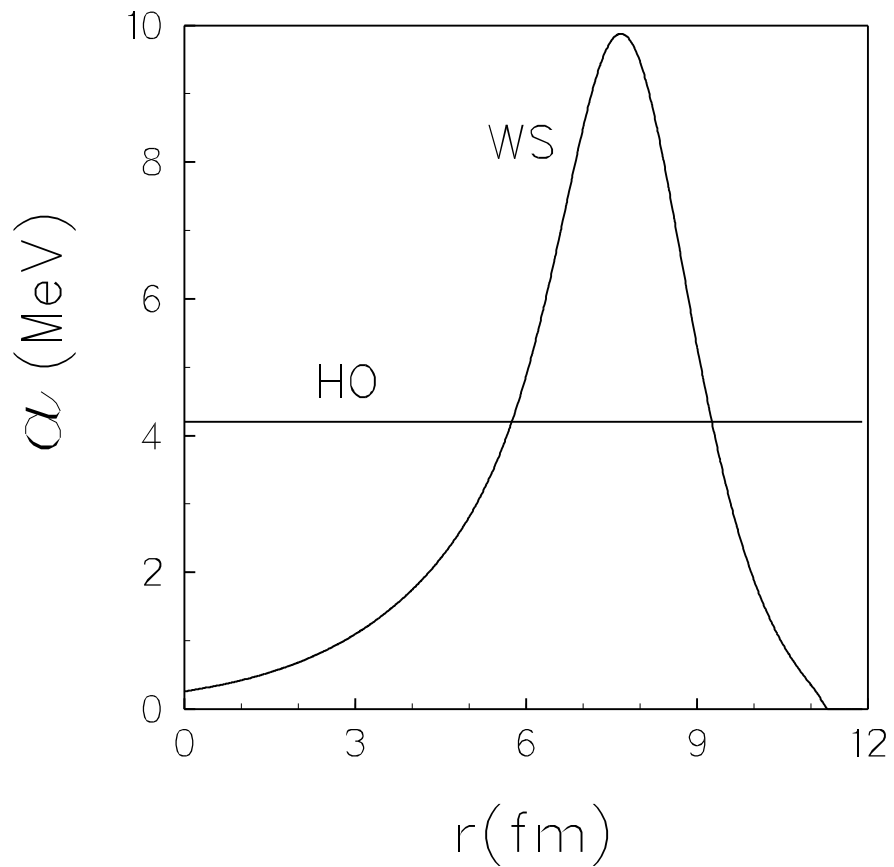


FIG. 9. The diffusivity parameter a of the equilibrium distribution function in momentum space as a function of the distance r to the center of the nucleus for both harmonic oscillator (curve HO) and Woods-Saxon (curve WS) potentials.

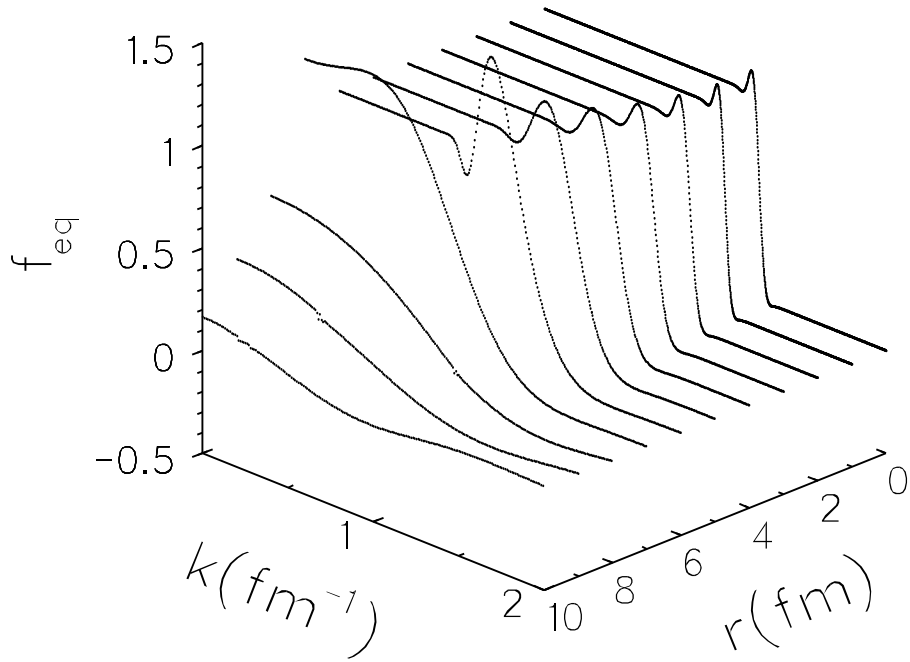


FIG. 10. The equilibrium distribution function in the WS potential as obtained from the semi-classical expansion on the Hermite polynomials Eq. (59), with $N = 3$.

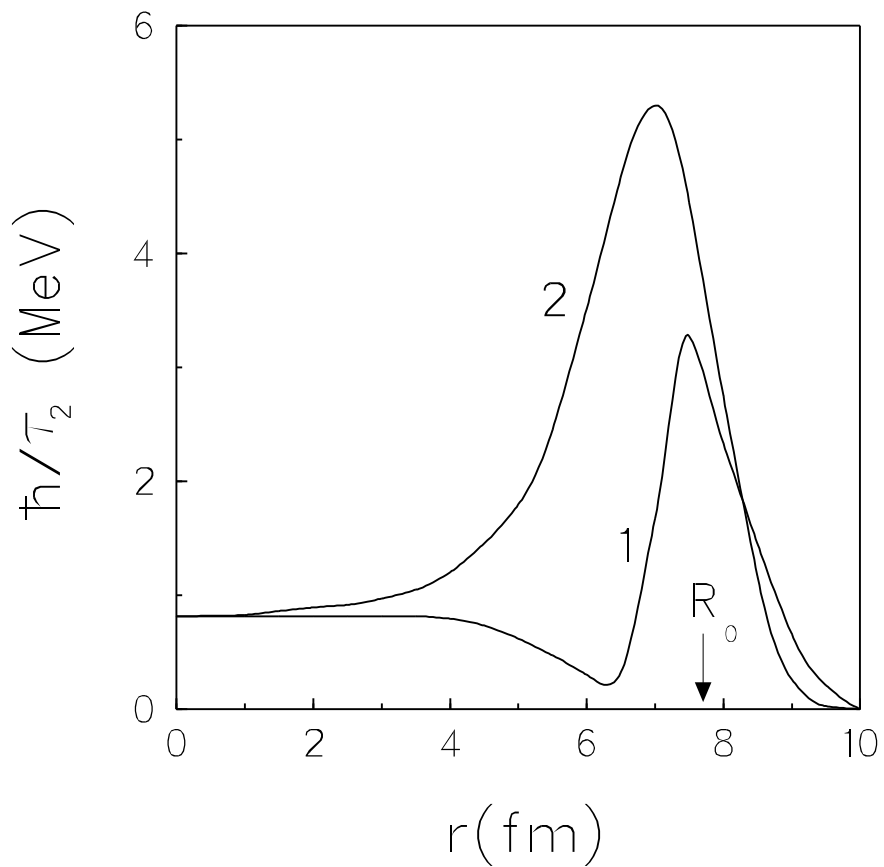


FIG. 11. The local damping parameter $\hbar/\tau_2(r, \omega_0)$ for the nucleus with $A = 224$, calculated for a spherical WS potential. For curve 1 we use the equilibrium distribution function (59) and for curve 2 we use the Fermi distribution function (60).

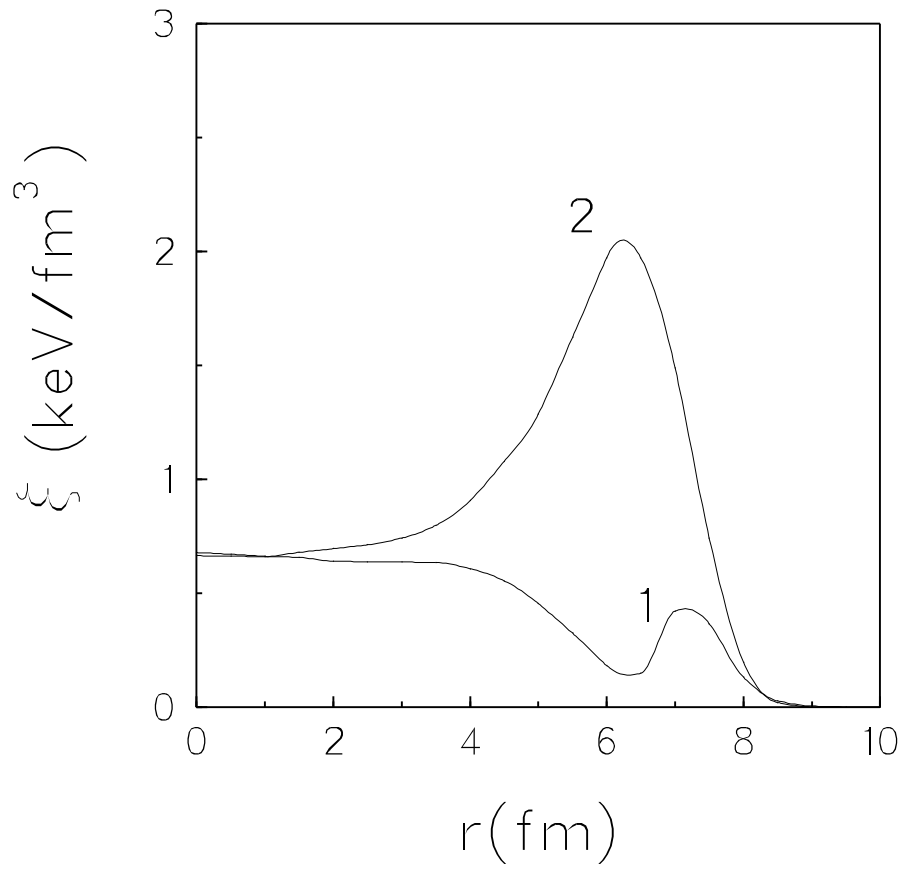


FIG. 12. The damping factor ξ in the case of the WS potential. The notations is the same as in Fig. 11.

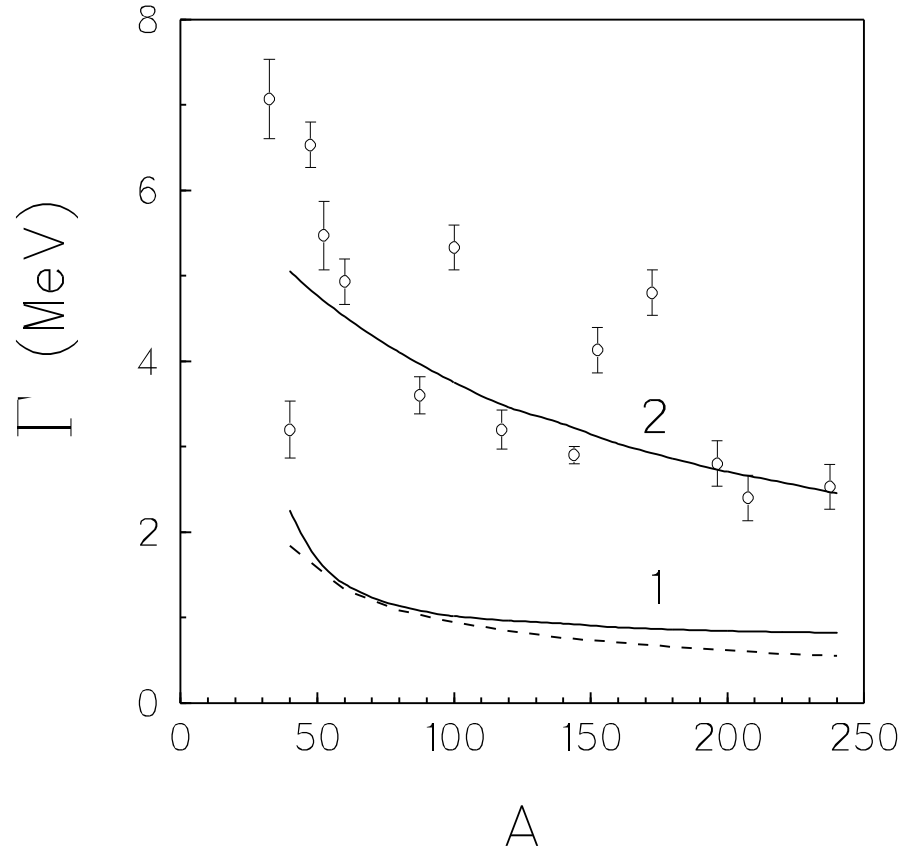


FIG. 13. The collisional width of the isoscalar giant quadrupole resonances obtained by using Eq. (40) with $\xi(r, \omega_0)$ from Fig. 12. The notations of curves 1 and 2 is the same as in Fig. 12. The dashed curve is from Fig. 8. The experimental data were taken from Refs. [31, 32].